ELSEVIER

Biophysical Chemistry 110 (2004) 171–178

Biophysical Chemistry

www.elsevier.com/locate/bpc

Packaging of single DNA molecules by the yeast mitochondrial protein Abf2p: reinterpretation of recent single molecule experiments

Dirk Stigter*

1925 Marin Ave, Berkeley, CA 94707, USA

Received 26 January 2004; accepted 27 January 2004
Available online 27 April 2004

Abstract

Brewer et al. (Biophys. J. 85 (2003) 2519–2524) have studied the compaction of dsDNA in a double flow cell by observing the extension of stained DNA tethered in buffer solutions with or without Abf2p. They use a Langmuir adsorption model in which one Abf2p molecule adsorbs on one site on the DNA, and the binding constant, K, is given as the ratio of the experimental rates of adsorption and desorption. This paper presents an improved interpretation. Instead of Langmuir adsorption we use the more appropriate McGhee–von Hippel (J. Mol. Biol. 86 (1974) 469–489) theory for the adsorption of large ligands to a one-dimensional lattice. We assume that each adsorbed molecule shortens the effective contour length of DNA by the foot print of Abf2p of 27 base pairs. When Abf2p adsorbs to DNA stretched in the flowing buffer solution, we account for a tension effect that decreases the adsorption rate and the binding constant by a factor of 2 to 4. The data suggest that the accessibility to Abf2p decreases significantly with increasing compaction of DNA, resulting in a lower adsorption rate and a lower binding constant. The kinetics reported by Brewer et al. (Biophys. J. 85 (2003) 2519–2524) lead to a binding constant $K=3.6\times10^6$ M^{-1} at the beginning, and to $K=5\times10^5$ M^{-1} near the end of a compaction run, more than an order of magnitude lower than the value $K=2.57\times10^7$ M^{-1} calculated by Brewer et al. (Biophys. J. 85 (2003) 2519–2524).

Keywords: Compaction of DNA; Adsorption to DNA; Accessibility of DNA; Binding constant of Abf2p

1. Introduction

Under biological conditions DNA occupies a space that is several thousand times smaller than the equilibrium volume of the dsDNA random coil in dilute solution. Various agents may condense or compact DNA in different ways. Brewer et al. [1] have studied the compaction of DNA by Abf2p, a protein found in the mitochondria of the yeast Saccharomyces cerevisiae. They measured extensions of single DNA molecules tethered in a bifurcated flow cell, thus allowing exposure of DNA stretched in flowing buffer solutions with

* Tel.: +1-510-526-4989.
E-mail address: stigter@maxwell.compbio.ucsf.edu (D. Stigter).

0301-4622/$ - see front matter © 2004 Elsevier B.V. All rights reserved.
doi:10.1016/j.bpc.2004.01.012

and without Abf2p. Compaction was measured in the protein solution followed by decompaction in the protein-free buffer solution. The extension data of the DNA were interpreted with a Langmuir model of the adsorption of Abf2p, assuming that one protein molecule may bind to one adsorption site on the DNA. This is a poor model because Abf2p does not adsorb at a single binding site. The footprint of Abf2p on DNA is approximately 27 base pairs (bp). So Abf2p occupies 27 bp, instead of 1 bp as implied by Brewer et al. [1]. Due to this error, their binding constant is a factor 27 too high. Other factors, also ignored by Brewer et al. [1], give further changes in the binding constant. This paper offers an improved interpretation. We address the following issues:

1. In Ref. [1] the adsorption of Abf2p is related to the extension of DNA. We convert the DNA extension to an effective contour length before evaluating Abf2p adsorption.
2. McGhee and von Hippel (M–H) [2] deal with multiple site adsorption of large ligands to a one-dimensional lattice such as dsDNA. We use the M–H theory for the Abf2p adsorption, whereas Ref. [1] uses M–H theory only to estimate maximum compaction.
3. In the experiments under discussion tethered DNA is under tension because it is stretched in the flowing solution. Adsorption of protein to DNA compacting under tension is more difficult than adsorption to relaxed DNA. We add in the adsorption equation a factor for this tension effect.
4. Ref. [1] treats adsorption to compacting DNA the same as to fully stretched DNA. However, compacting DNA becomes less accessible to the Abf2p in solution, so the adsorption rate decreases.
5. Brewer et al. [1] evaluate a protein binding constant as the ratio of the experimental rates of adsorption and desorption. This gives a binding constant which is at least an order of magnitude too high.

2. Compaction experiments and effective contour length of DNA

The bifurcated flow cell allows a buffer solution and a buffer+Abf2p solution to move side by side at the same velocity. A stained DNA molecule, attached at one end to a 1 μm bead held in an optical trap, is first stretched in the buffer solution and its extension is measured. Then the optical trap, holding the bead at one end of the DNA, is moved sideways into the Abf2p solution. Here one observes the shortening (compaction) of the DNA to an equilibrium extension, which is approached about exponentially in time. When the DNA is moved back to the buffer solution, it lengthens (decompacts) exponentially in time to the earlier extension.

Figs. 1 and 2 show the compaction of DNA in buffer+1.43 μM Abf2p solution and subsequent decompaction in buffer solution. The crosses (lower points) are the observed extensions. In each case, the diamond is the contour length calculated (see below) from the extension and the relevant flow velocity.

Perkins et al. [3] developed the technique of stretching a tethered DNA molecule in a solution flowing past it. Zimm [4] and Stigter and Bustamante [5] published quantitative theories. The theories differ somewhat in hydrodynamic detail, but both agree well with the experiments [4,5], essentially without using adjustable parameters. We summarize the theory of Stigter and Bustamante [5] which we apply to the experimental extensions in Figs. 1 and 2 to find the relevant contour lengths.

We use the freely jointed chain model in which the DNA chain is divided into N ellipsoidal Kuhn segments, each with length $2P$ where P is the persistence length of the chain. The DNA is tethered at segment N and extends to segment 1 at the free end. In steady state extension, the elastic tension force in each segment i=1 to N is balanced by the viscous drag (stretching force) on the chain between segment i and the free end of the chain. The theory for the entropic elasticity of worm-like polymer chains [6] yields the relation between the tension in a segment and its orientation, which is given by the angle θ between the axis of the segment and the z-axis, which is the direction of flow. A second coordinate for each segment, the randomly chosen angle of rotation of the segmental axis around the z direction, completes the conformation of the freely jointed chain. For hydrodynamic purposes each ellipsoidal segment, including its orientation, is represented by an equivalent Stokes sphere. The pairwise hydrodynamic interaction between the N spheres depends on the geometry of the chain. So we have one mechanical

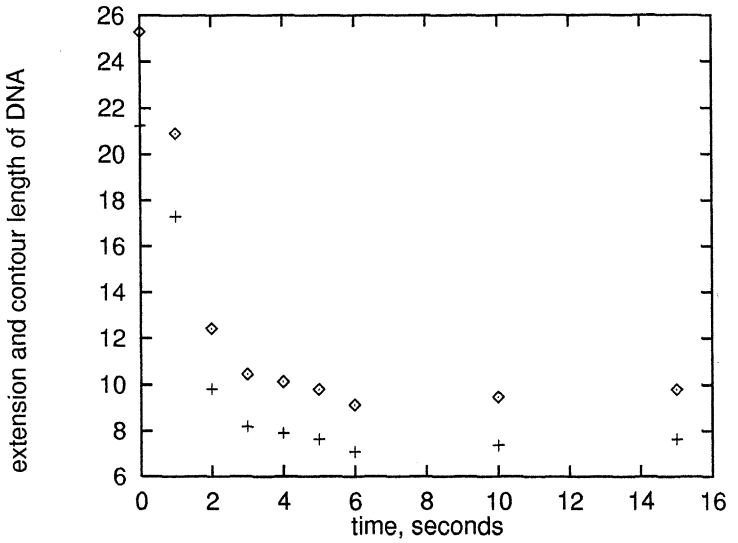

Fig. 1. DNA first stretched in buffer solution (not shown) compacts in buffer+1.43 μM Abf2p solution, starting at time t=0. Flow velocity 104 μm/s. Crosses: experimental extensions, μm. Diamonds: calculated effective contour lengths, μm. Experiments by Brewer et al. [1].

equilibrium equation between elastic tension and viscous drag forces for each segment i. These N equations are interrelated through the hydrodynamic interaction effects, which depend on chain conformation. A well instructed computer is needed to deal with these equations.[1] Iteration yields a selfconsistent solution which includes the angles with the z-axis, θ_i, for segments i=1 to N. This gives the steady state extension E of the chain in the flow direction

$$E = 2P\sum_{i=1}^{N}\cos,\ \theta_i \tag{1}$$

as a function of its contour length L=2PN.

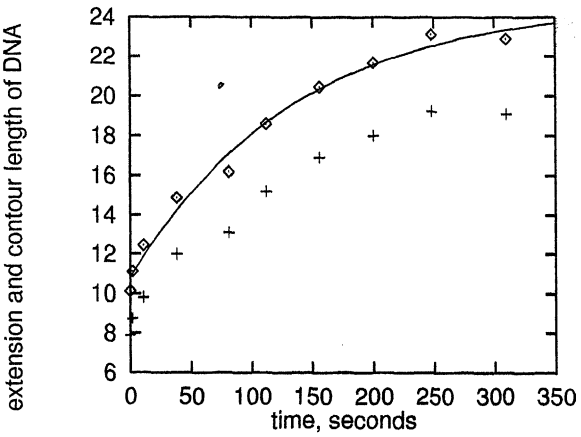

Fig. 2. Decompacting of DNA after transfer from Abf2p into the buffer solution at time t=0. Flow velocity 104 μm/s. Crosses: Experimental extensions, μm. Diamonds: calculated effective contour lengths, μm. Solid curve: best exponential fit to diamonds, $24.74-13.95e^{-kt}$ with k=0.0074±0.0013 s^{-1}. Experiments from Brewer et al. [1].

In the present experiments the DNA was stained with YOYO-1, one molecule intercalated per 10 to 15 base pairs. For such stained DNA in buffer solution we assume a persistence length P=550 Å, with relevant smaller values for compacted segments.[2] Fig. 3 shows the relative extension, E/L, vs. the contour length for the flow velocity of Figs. 1 and 2. An iteration procedure using Eq. (1) yields L from E. In this way

[1] To prevent divergence of the iteration procedure, in particular for highly compacted DNA, instructions are included to avoid positive tension gradients and the overlap of Stokes spheres.

[2] The friction factor of a compacting chain segment decreases because the segment becomes shorter, and increases because of adsorption of Abf2p. Assuming that these changes cancel each other, we use for all segments the friction factors in the uncompacted DNA.

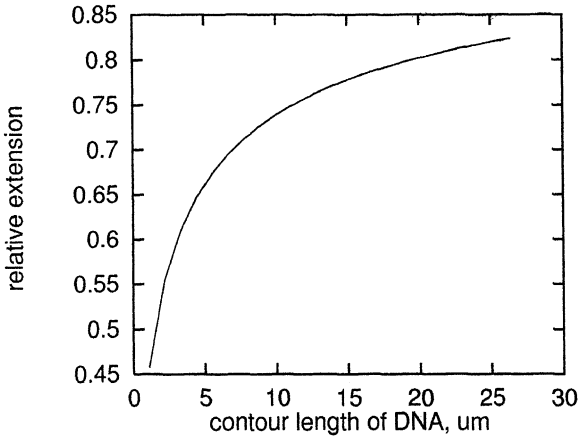

Fig. 3. Ratio of extension and contour length as a function of the contour length of DNA, μm. Flow velocity 104 μm/s.

the contour lengths (diamonds) in Figs. 1 and 2 were obtained from the relevant extensions (crosses).[3]

3. Compaction and adsorption to relaxed DNA

Experiments by Brewer et al. [1] show that compaction and decompaction are slow enough for hydrodynamic steady state conditions to prevail. Compaction of DNA is connected to the adsorption of Abf2p protein by assuming that each adsorbing protein molecule shortens the effective contour length L of DNA by its footprint of n=27 bp. Protein may adsorb along the entire length of the DNA chain in a dynamic binding process. Equilibrium is reached when the rates of deposition (adsorption) and release (desorption) are equal. We define the adsorption density v as the number of adsorbed proteins per base pair, $0 \le v \le 1/n$.

It is straightforward to connect the rates of desorption and decompaction. In Fig. 2 we start from the compacted state at t=0 and finish in the equilibrium extended state at $t=\infty$. We indicate these states by subscripts c (for compacted) and b (for buffer). The in-between states carry no subscript. The effective contour length L during compaction or decompaction is

$$L = L_b(1-n) \tag{2}$$

At time t=0 desorption starts from the adsorption density v_c corresponding to the effective contour length

$$L_c = L_b(1-n_c) \tag{3}$$

When b is the contour length per base pair, the number of Abf2p molecules bound per chain is $(L_b/b)v$. The desorption rate, $(L_b/b)\mathrm{d}v/\mathrm{d}t$ molecules per second, is the number of bound molecules per chain multiplied by the rate per bound molecule, k_d, that is,

$$\frac{L_b}{b}\frac{\mathrm{d}v}{\mathrm{d}t} = -\frac{L_b}{b}vk_d \tag{4}$$

Integration of Eq. (4) and applying Eq. (3), the conditions at t=0 and $t=\infty$ yield

$$L = L_b - (L_b - L_c)e^{-k_d t} \tag{5}$$

Comparison with Fig. 2 shows that k_d=0.0074±0.0013 s^{-1}.

We proceed with the adsorption and compaction in Fig. 1, starting with the adsorption to relaxed DNA at very low density v. In that case, the rate of adsorption per DNA molecule is proportional to the concentration c of Abf2p in solution, and to the number of unoccupied base pairs, (L_b/b) $(1-nv)$, multiplied by k_a, the intrinsic adsorption rate in molecules per base pair per second. There is an extra contribution from the ongoing desorption, as in Eq. (4), so that the net rate of adsorption is

$$\frac{L_b}{b}\frac{\mathrm{d}v}{\mathrm{d}t} = \frac{L_b}{b}(1-nv)ck_a - \frac{L_b}{b}vk_d \tag{6}$$

Apart from a different notation, Brewer et al. [1] interpret their compaction experiments with Eq. (6), assuming n=1. (The signs on the rhs of Eq. (1) in Ref. [1] should be reversed.)

[3] In a second computation the number N of segments in the chain was reduced while their length $2P$ was kept constant. The results for the effective contour length differed less than 0.12 μm from those for the diamonds in Figs. 1 and 2. This shows that the effective contour length is very insensitive to the assumed value of the persistence length, not unexpected for chains under stretching conditions.

Adsorption equilibrium is reached for $dv/dt=0$, when release of protein equals deposition. For this binding equilibrium

free protein binding sites + free protein⇌bound protein

$$L_b(1-nv)/b \qquad c \qquad L_b v/b \tag{7}$$

it is conventional to define the binding constant with the mass-action equation

$$K = \frac{L_b v/b}{L_b(1-nv)c/b} = \frac{v}{(1-nv)c} \tag{8}$$

Comparison with Eq. (6) for $dv/dt=0$ shows that

$$K = k_a/k_d \tag{9}$$

Integration of Eq. (6) gives the adsorption as a function of time. With $v=0$ for $t=0$ we find

$$v = \frac{k_a c}{nk_a c + k_d}\left(1 - e^{-(nk_a c + k_d)t}\right) \tag{10}$$

The experimental adsorption rate, k_{on}, used by Brewer et al. [1] is about a factor n greater than k_a and, hence, their binding constant would be a factor $n=27$ too large. However, there are more issues involved.

Eq. (6) is valid only for an essentially empty lattice of DNA sites. For significant occupation only a fraction of the empty sites is available for further adsorption, that is, the fraction in stretches of at least $n=27$ empty sites. This excluded volume effect leads to decreased adsorption rates, given by the extra factor [2,7]

$$g(v) = \left(\frac{1-nv}{1-(n-1)v}\right)^{n-1} \tag{11}$$

Desorption does not suffer from excluded volume effects.

4. Adsorption of Abf2p to DNA under tension

Adsorption to DNA under tension is more difficult than the adsorption to relaxed DNA discussed so far. Fig. 4 shows schematically stretched DNA in buffer+ Abf2p solution, and an expanded view of a single chain segment i under tension T_i, under an angle θ_i with the z axis, before and after adsorption of an Abf2p molecule.

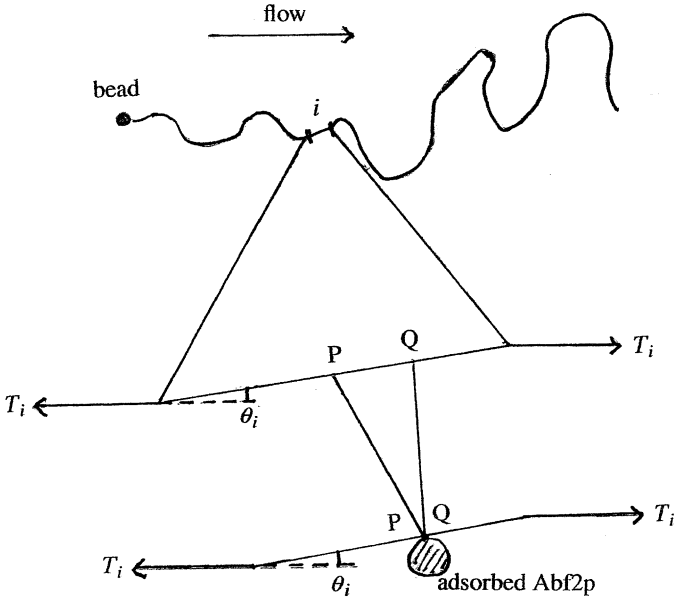

Fig. 4. Schematic adsorption of Abf2p to DNA stretched in flow.

The adsorption shortens the chain segment by the length PQ=nb against the tension force $T_i\cos\theta_i$. This reduces the binding energy per Abf2p molecule by

$$u_i = nbT_i\cos\theta_i \tag{12}$$

We account for this change by multiplying for every chain segment the intrinsic adsorption rate by the Boltzmann factor $e^{-u_i/kT}$. Along with the excluded volume factor $g(v)$ from Eq. (11), we add this tension factor explicitly in the expressions below, using for k_a the value for relaxed DNA when $v\rightarrow 0$. The intrinsic desorption rate is not changed by the tension so the Eqs. (4) and (5) are still valid. Instead of Eq. (6) we now have for each segment with L_b/Nb base pairs

$$\frac{L_b}{Nb}\frac{dv_i}{dt} = \frac{L_b}{Nb}(1-nv_i)ck_a e^{-u_i/kT}g(v_i) - \frac{L_b}{Nb}v_i k_d \tag{13}$$

Dividing by L_b/Nb and averaging over all segments Eq. (13) yields

$$\frac{dv}{dt} = ck_a\left\langle e^{-u_i/kT}(1-nv_i)g(v_i)\right\rangle - vk_d \tag{14}$$

where $\langle\rangle$ indicates the chain average. For adsorption equilibrium, when $v=v_c$ and $dv/dt=0$, Eq. (14) gives for the binding constant

$$K = \frac{k_a}{k_d} = \frac{v_c}{c\left\langle e^{-u_i/kT}(1-nv_i)g(v_i)\right\rangle_c} \tag{15}$$

where the average over all segments i in the compacted chain is indicated by $\langle\rangle_c$. For relaxed DNA, with $u_i=0$ and $v_i=v$ for all segments i, Eq. (15) for K is consistent with Eq. (10) of McGee and von Hippel [2].

5. Decreased accessibility of compacted DNA to Abf2p

Eq. (14) cannot be integrated analytically to find the change of effective contour length with time, and compare with the compaction kinetics in Fig. 1. Therefore, we have applied a numerical procedure that assumes that at any moment the chain compaction is determined by the Abf2p adsorption at all segments. This is consistent with our basic assumption connecting the effective contour length and Abf2p adsorption. We carry out the numerical integration of the N Eq. (13) in small time steps Δt. At $t=0$, we start with known values $v_i=0$ and u_i for all i. After time Δt, Eq. (13) gives a new set of v_i values. This is input for solving the set of N interrelated hydrodynamic stretch equations to find the new values of the tensions T_i and, with Eq. (12), the new energies u_i. In this way the v_i's and the u_i's are updated alternatively after each time step, giving with Eqs. (14) and (2), the desired adsorption and compaction kinetics.

The dashed curves in Fig. 5 show results for the effective contour length from two numerical integrations of the adsorption/compaction kinetics, for $k_a=1.26\times10^4$ M^{-1} s^{-1} (upper dashed curve) and for $k_a=5\times10^4$ M^{-1} s^{-1} (lower dashed curve). There are some obvious discrepancies between the dashed curves and the diamonds in Fig. 5. Fitting the experimental adsorption kinetics with Eq. (14) would require a progressively lower k_a value when compaction proceeds, from $k_a=5\times10^4$ M^{-1} s^{-1} at the start to a much lower k_a value towards the end of the compaction process.

A simple explanation is that the compaction of DNA impedes the adsorption of ABF2p. The values of k_a, k_d, and K are mainly determined by short range forces that do not vary with DNA compaction. Therefore it is likely that the flow of Abf2p toward the DNA surface is hindered by compaction, thus decreasing the rate of adsorption. One might describe this hindrance by a decreased (effective) Abf2p concentration. However, such a quantity would be difficult to determine experimentally. Therefore, we absorb the effects of decreased accessibility of compacted DNA in lowered values of the adsorption rate k_a. In the beginning of the compaction process, when the DNA is still fairly open and accessible, one expects little effect on the adsorption flow, but toward the end the hindrance should be maximal when mainly the outside surface of the compacted DNA molecule is accessible. In Fig. 6 this is represented schematically by a linear decrease from $k_a=5\times10^4$ M^{-1} s^{-1} for low compaction to the

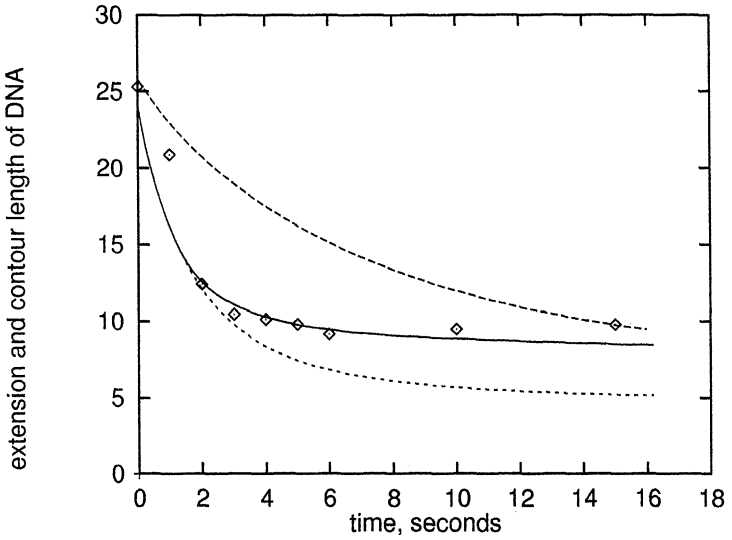

Fig. 5. Test of adsorption/compaction kinetics of experiments of Fig. 1 with Eqs. (13) and (14) and c=1.43 μM. Diamonds: Effective contour length, μm, from Fig. 1. Dashed curves: from numerical integration of adsorption, with k_a=1.26×10^4 M^{-1} s^{-1} (upper curve) and k_a=5×10^4 M^{-1}s^{-1} (lower curve). Solid curve: From numerical integration of adsorption with k_a from Fig. 6.

smaller value k_a=0.7×10^4 M^{-1} s^{-1} for high compaction. Integrating Eq. (13) with k_a from Fig. 6 yields the solid curve in Fig. 5, in good agreement with the diamonds from experiments.

6. Binding constant of Abf2p

Desorption of Abf2p is not influenced by the compaction of DNA. Brewer et al. [1] determined

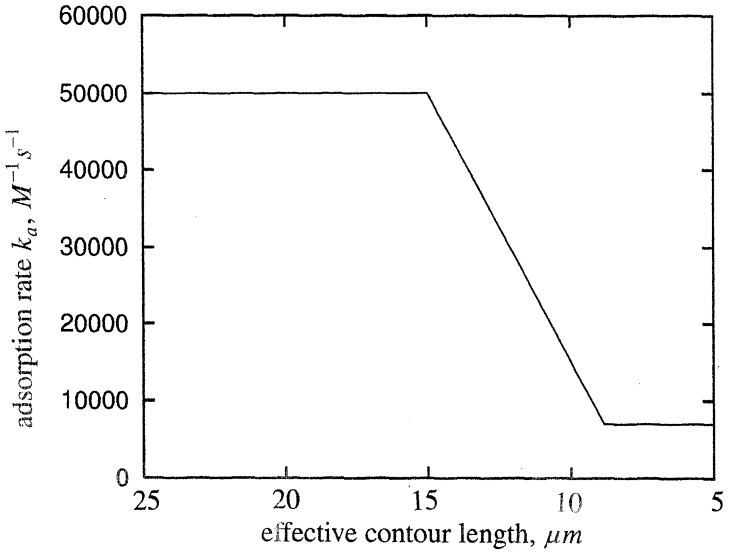

Fig. 6. Schematic adsorption rate of Abf2p, k_a, to compacting DNA vs. effective contour length, μm.

decompaction rates for 10 molecules, reporting an average rate of 0.014 s^{-1}. Fig. 2 shows that the difference between the rates of decompaction (crosses) and desorption (diamonds) is small. Here we neglect the difference and use for the desorption rate k_d=0.014 s^{-1}. With the adsorption rates from Fig. 6; Eq. (9) yields for the binding constant $K=5\times10^4/0.014=3.6\times10^6$ M^{-1} at the start of compaction, down to $K=0.7\times10^4/0.014=5\times10^5$ M^{-1} near the end of compaction. This compares with $K=2.57\times10^7$ M^{-1} calculated by Brewer et al. [1].

In equilibrium experiments K depends only on the accessibility of DNA in the equilibrium compacted form. Also in general, the effect on K is larger than the (average) effect on k_a. The equilibrium compaction data in Fig. 3 of Ref. [1] show a large spread, mostly due to the uncertainty in buffer flow velocity, 80±30 μm/s. From accurate compaction experiments, one could determine values of the binding constant K with the McGhee–von Hippel theory corrected for the tension effect in stretched DNA. From such equilibrium experiments, we predict results for K that are in the neighborhood of $K=5\times10^5$ M^{-1}, as calculated above from kinetic experiments for high compaction.

For the solid curve in Fig. 5 we have estimated the tension effects on k_a and on K. We find values for $\left\langle e^{-u_i/kT}\right\rangle$ from 0.28 to 0.58. This shows that adsorption of Abf2p to stretched DNA is approximately 2–4 times slower than to relaxed DNA. In addition, binding constants to relaxed DNA should be 2–4 times greater than to stretched DNA.

For 25-μm long DNA stretched in 104 μm/s flow, solid line in Fig. 5, we calculate a tether force of 0.84–1.84 pN. This compares with a mean tether force of 0.6 pN reported by Brewer et al. [1] for 5–15 μm long DNA stretched in unspecified liquid flow velocity.

References

[1] L.R. Brewer, R. Friddle, A. Noy, E. Baldwin, S. Martin, M. Corzett, et al., Packaging of single DNA molecules by the yeast mitochondrial protein Abf2p, Biophys. J. 85 (2003) 2519–2524.

[2] J.M. McGhee, P.H. von Hippel, Theoretical aspects of DNA–protein interactions: co-operative and non-cooperative binding of large ligands to a one-dimensional homogeneous lattice, J. Mol. Biol. 86 (1974) 469–489.

[3] T.T. Perkins, D.E. Smith, R.G. Larson, S. Chu, Stretching of a single tethered polymer in uniform flow, Science 268 (1995) 83–87.

[4] B.H. Zimm, Extension in flow of a DNA molecule tethered at one end, Macromolecules 31 (1998) 6089–6098.

[5] D. Stigter, C. Bustamante, Theory for the hydrodynamic and electrophoretic stretch of tethered B-DNA, Biophys. J. 75 (1998) 1197–1210.

[6] J.F. Marko, E.D. Siggia, Stretching DNA, Macromolecules 28 (1995) 8759–8770.

[7] K.A. Dill, S. Bromberg, Molecular Driving Forces, Garland Science, New York, 2003, p. 552f.